Theor Chem Acc (2000) 104:302–311
DOI 10.1007/s002140000123

Theoretical
Chemistry Accounts

Regular article

Hydrogenation of acetylene–ethylene mixtures on Pd catalysts: study of the surface mechanism by computational approaches. Metal dispersion and catalytic activity

Dario Duca[1], **Zsuzsanna Varga**[1], **Gianfranco La Manna**[2], **Tamás Vidóczy**[3]

[1] Dipartimento di Scienze Farmaceutiche, Università, Via Ponte don Melillo, 84084 Fisciano, Salerno, Italy
[2] Dipartimento di Chimica Fisica, Università, Viale delle Scienze, 90128 Palermo, Italy
[3] Central Research Institute for Chemistry, Hungarian Academy of Sciences, Pusztaszery út. 59-67, 1025 Budapest, Hungary

Received: 16 September 1999 / Accepted: 3 February 2000 / Published online: 2 May 2000

Abstract. The hydrogenation mechanism of acetylene–ethylene mixtures on Pd catalysts under different experimental conditions was studied by employing a time-dependent Monte Carlo approach set to use a fixed series of event probabilities. The dependence of the catalyst activity and selectivity on the sizes of the metal particles was simulated at microscopic level and the results, also refined by fitting procedures, suggested proper explanations for the apparent nonuniformity of the related experimental findings. The use of the steric hindrance parameter of the surface species and the available surface energy on the metallic catalyst sites was decisive for reproducing the experimental results.

Key words: Time-dependent Monte Carlo – Acetylene-ethylene mixture hydrogenation

1 Introduction

Selective hydrogenation of alkynes and alkadienes in alkene-rich feedstocks is a crucial preliminary step in polymer synthesis. The removal of unsaturated hydrocarbons from the mixtures, to reach a few parts per million, is required to avoid poisoning effects on the polymerisation catalysts. Selective hydrogenation of acetylene traces in ethylene-rich feedstocks containing hydrogen amounts comparable either with that of ethylene [1] (front-end mixtures) or with that of acetylene [2] (tail-end mixtures) is currently an important industrial target [3]. The resulting products of this preliminary transformation are employed in polyethylene synthesis. For this reason the wastage of ethylene must be limited. With this aim, low-charged Pd on amorphous alumina catalysts was developed and is still widely used today. Besides the practical aspects, the apparent simplicity of the mechanism involved in acetylene hydrogenation stimulated the use of this reaction as a model reaction and consequently much has been published on this topic.

Even the influence of the metal particle size on the activity of heterogeneous metal catalysts has been greatly debated [4] in recent years. Indeed, this aspect was considered for both academic and practical purposes [5] in order to gain more understanding about the mechanism and to improve catalyst activity, respectively. Other factors, such as surface decoration effects [6], may, however, affect the reactivity of the metal catalyst. Decoration effects could arise from the growth characteristics of the metallic crystallite and/or the formation of surface deposits [7, 8] occurring with the catalytic reaction. Of course, experimentally it is impossible not to have convoluted outcomes; therefore, it is not simple to understand the real influence of the particle size and of the surface decoration effects on the reaction mechanism. The study of these influences is further complicated by the fact that they can originate both by geometric and/or electronic effects.

In fact, the mechanism of acetylene–ethylene hydrogenation on metal catalysts turned out not to be at all simple and was characterised by broken up insights [5–9]. Hence, different surface mechanisms have been suggested for different experimental conditions.

A model employing a deterministic algorithm has been tried to unify the different perspectives on the reaction mechanism [7]. In this case, however, the generality of the result was strongly affected by the characteristics of the deterministic approach [10] employed.

Here, it is shown that the time-dependent Monte Carlo (tdMC) method [11, 12] is able to reproduce the intrinsic details of the title reaction and to evaluate the relevance of the surface dynamics involved. The stochastic model presented in this work was tested by simulating various experimental aspects of acetylene–ethylene hydrogenation. The different experimental as-

Correspondence to: D. Duca
e-mail: dduca@unisa.it

pects were framed as one surface mechanism defined by elementary microscopic events drawn by predetermined [12] probabilities of occurrence.

Here a study concerning the influence of the crystallite sizes on the activity and selectivity of the Pd catalysts employed in the title reaction is performed together with an introduction to the chemical model employed and to technical and computational details.

2 Platforms, reaction model, codes and other technical aspects

Several Pentium II (266–450 MHz) personal computers and one Digital Alpha (500 MHz) work station were employed in this work. In the fitting procedures they were connected by a virtual parallel technique employing the PVM3 algorithm [12]. Identical results were obtained in the simulations irrespective of the platform used.

The tdMC algorithm is based on the Ziff, Gulari, Barshad (ZGB) model [13]. Like the latter, it does not need to explicitly consider any expression of interaction potential because the occurrence probabilities of the different events (see later) are fixed before starting the simulations; however, in contrast to the ZGB algorithm, tdMC is able to perform a direct comparison with experimental kinetics results. This is because it includes an internal clock characterised by a time unit tuned with the frequency of the faster simulated event [10, 11], that is determined automatically by the present code.

In the following we will refer to different time definitions:

- Simulation time, processing time to perform a given simulation.
- Step time, time unit considered in a given simulation. Time is incremented by one step for any hit of hydrogen on the surface.
- Reaction time, experimental time reproduced in a given simulation.
- Time slice, any considered fractions of the reaction time.
- Event time, a nonconstant time slice elapsing between two sequential events.

In the reaction model it is hypothesised that the macroscopic effects produced by the title reaction, which we suppose to occur in a continuous flow reactor [7], are determined by the following elementary events:

- Null event, i.e. nothing occurs in the event time.
- Dissociative adsorption on and desorption from the Pd surface of molecular hydrogen.
- Diffusion of atomic hydrogen through the Pd surface.
- Adsorption on, diffusion through and desorption from the Pd surface of acetylene, ethylene and ethane.
- Formation on the Pd surface of molecular hydrogen, ethyl, ethylene, vinyl and ethane by the meeting of atomic hydrogen and the complementary surface species.
- Diffusion through the Pd surface of vinyl or ethyl.
- Removal from the Pd surface of vinyl or ethyl with the formation of atomic hydrogen and acetylene or ethylene, respectively.
- Formation on the Pd surface of carbonaceous species (i.e. polymer species) having various shape and steric properties.

All of these events have their own occurrence probability (see later). As the events are mutually independent, the sum of the event probability values, including the null event, was never allowed to exceed 1 during the simulation. A simplistic chemical representation of the above points is given in the following Horiuti–Polanyi-like scheme:

$$
\begin{aligned}
&H_2 + 2* \Leftrightarrow 2H(*)\\
&C_2H_2 + 2* \Leftrightarrow C_2H_2(*)_2\\
&C_2H_4 + 2* \Leftrightarrow C_2H_4(*)_2\\
&C_2H_6 + 2* \Leftrightarrow C_2H_6(*)_2\\
&C_2H_2(*)_2 + H(*) \Leftrightarrow C_2H_3(*)_2 + *\\
&C_2H_4(*)_2 + H(*) \Leftrightarrow C_2H_5(*)_2 + *\\
&C_2H_3(*)_2 + H(*) \Rightarrow C_2H_4(*)_2 + *\\
&C_2H_5(*)_2 + H(*) \Rightarrow C_2H_6(*)_2 + *\\
&C_xH_y(*)_m + C_wH_z(*)_n \Rightarrow C_{(x+w)}H_{(y+z)}(*)_{(m+n)} \ ,
\end{aligned}
$$

where $*$ and $(*)$ represent empty and occupied surface sites, respectively, and $X(*)_n$ generic species X adsorbed on n adjacent catalyst sites. Among the possible atomic surface hydrogen [14], the $H(*)$ considered in this work are the less thermodynamically stable surface hydrogen species, with the others not actually participating in the reaction [12]. The catalyst surface was mimicked by square matrices [10, 12], representing {100} Face-centred cubic metal faces, having sizes ranging between 50×50 and 100×100 elements (i.e. surface sites). Diagonal movements through the surface are therefore not allowed to the reacting species; however, this did not influence the simulation results [12, 15]. Periodic boundary conditions and lateral interactions were introduced [12] to perform the simulations.

Since the simulations were performed for reactions occurring in a continuous flow reactor, to consider the changes of the number of molecules in the vapour phase is not essential. In fact, the tdMC algorithm is able to keep a constant composition of the mixture in the gas phase, as derived from the conditions that were imposed in the experiments.

The choice of the metallic face, the matrix sizes and the other points mentioned previously ensured an acceptable simulation time and the ability to reproduce the mimicked physical conditions.

Simulating reactions that occur [7] in a continuous-flow fixed-bed reactor, the composition of the vapour phase was not influenced by ethane and/or ethylene formation; therefore, the readsorption of ethane was not taken into consideration. Since the experimental hydrocarbon conversion values were very low [7], the conditions relative to the composition of the vapour phase were actually realistic.

The self-written tdMC algorithm employed in the work is an expanded version of that used in the study of ethylene hydrogenation [12] on metallic catalysts. RAN2 from Ref. [16] was used as a portable random number generator.

Taking into consideration the independence of the events, they had a different starting seed and, therefore, a different set of generated random numbers. The results did not change significantly on carrying out simulations that differed only for the set of starting seeds [10, 12].

The typical reaction time reproduced in the simulation was fixed at 1.0×10^{-3} s because it is certainly quite longer than the time necessary to reach the steady state. Moreover, the step time values were in the range between 1.0×10^{-11} and 1.0×10^{-12} s, depending on the gas-phase mixture considered. These values were chosen to obtain total probability values lower than 1. Since in every step 10^2–10^3 sequential events occurring in a time slice having values within limits of 1.0×10^{-13}–1.0×10^{-15} s (event times) were considered, 10^{11}–10^{12} events were mimicked in the whole simulation.

The averaged values of the surface molar ratio of the different species were collected in 205 points along with the corresponding averaged values of the catalyst activity and selectivity (see later). Therefore, every point, representing an averaged value of a given physical property (e.g. the surface molar ratio), was determined by the contribution of about 5×10^8–5×10^9 values of the same property sequentially taken in a corresponding time slice. This time slice had a typical value of 9.8×10^{-6} s. In particular, diagrams of the surface population versus time slice were employed to establish [10, 12] transient and steady-state conditions of the reaction.

In this work, the results, obtained by simulating different experimental conditions, were compared only when the surface reaction reached [12] a steady state.

The catalyst activities for the conversions $C_2H_2 \rightarrow C_2H_4$ and $C_2H_4 \rightarrow C_2H_6$ were reported by their statistical equivalent [12] of the turnover frequency, $TOF_{C_2H_4}$ and $TOF_{C_2H_6}$, respectively. The selectivity was defined as the selectivity to ethane, S_E [7]. At a given time slice, the selectivity to ethane is defined as

$$S_E = \frac{\text{Number of molecules of ethane formed}}{\text{Number of molecules of acetylene converted}} \times 100 = \frac{TOF_{C_2H_6}}{TOF_{C_2H_4}} \times 100 \quad (1)$$

S_E was introduced into the study of acetylene hydrogenation in ethylene-rich feedstocks for technical reason [17]; in contrast to the usual definitions of selectivity, the lower the value of S_E, the better the selectivity of the catalyst. Experimental and simulated TOF and selectivity to ethane are considered in this work. Since there is no contest in which confusion can be induced, the same symbols ($TOF_{C_2H_4}$, $TOF_{C_2H_6}$ and S_E) will be employed for experimental and simulated data.

Event probabilities are obtained [12] using the equation $P = f\Delta tL$, where f is the frequency of occurrence per site per second of a given event, Δt is the step time and L is the number of surface sites considered in the simulation. The values of f are determined by collision theory for the adsorption processes and by transition-state theory for all other actions.

The frequency of the adsorption processes is given by

$$f = c\frac{\sigma_T p_x f(\theta)}{\sqrt{2\pi m_x k_B T}} \quad . \quad (2)$$

Referring to species X, σ_T is the sticking probability of this species on free surface sites at a given temperature T; p_x and m_x are the partial pressure and molecular mass of X and k_B is the Boltzmann constant. The function $f(\theta)$ is continuously updated by the tdMC algorithm [10, 12] and depends on the surface population. c is the surface of one site, here set equal to πr^2, with r the atomic radius of the metallic site. The frequency of the other events is given by

$$f = (k_B T/h) f(Q) \exp(-\Delta E/k_B T) f(\theta) \quad , \quad (3)$$

where h is the Planck constant, ΔE the activation energy of the process and $f(Q)$ is a functional expression of the partition functions of the reactants and the activated complex involved in the elementary event. In our surface reaction model $f(Q)$ can be estimated to be 1 for all the events [12, 18] considered.

The steric hindrance parameter [10, 12] of the molecules involved in the surface reaction was taken into account in the simulation and its role was crucial to achieve good reproduction of the experimental results. The values of the steric hindrance parameters of the surface species are summarised in Table 1, whereas the thermodynamic parameters employed to determine [12] the event frequencies are reported in Tables 2 and 3. If not explicitly underlined these thermodynamic parameters were employed to calculate the event probabilities used in the simulations reported in this work.

Adsorption–desorption [23] processes of acetylene and ethylene and their hydrogenation, at the very beginning of the reaction, on Pd and/or Pt surfaces have very similar rates. For this reason, to reduce the number of parameters to be used in the simulation, we employed in the hydrogenation–dehydrogenation steps of C_2H_2 and C_2H_4 on Pd the same values of the activation energies found [12] for the hydrogenation–dehydrogenation steps of C_2H_4 on Pt. In the mimicked experiments, in contrast to the steric hindrance parameters, that were kept fixed, the partial pressure of the reagents and the

Table 1. Steric hindrance parameter (*SHP*) of the surface species involved in the catalytic hydrogenation of acetylene–ethylene mixtures on Pd catalysts. The values of the SHP show qualitative agreement with ab initio quantum mechanical calculations [12, 19] related to interaction energy of pairs of species

Surface species	10 SHP
H	10[a]
C_2H_2	2.5[b]
C_2H_3	1.5[c]
C_2H_4	0.5[b]
C_2H_5	0.5[d]
C_2H_6	0.5[d]

[a] Surface hydrogen as the empty surface sites do not have any steric hindrance [10, 12]
[b] Determined by the Monte Carlo approach [12], reproducing experimental findings of surface population at equilibrium [20]
[c] Obtained by averaging acetylene and ethylene SHP
[d] From time-dependent Monte Carlo simulation [12]

Table 2. Sticking probabilities of molecules on free sites at 298 K and the activation energies employed to determine the adsorption frequency, per second per site, involved in catalytic acetylene–ethylene hydrogenation on Pd catalysts

Process	$100\sigma_{298}$ [a]	$\Delta E_{ads}/100$ (kJ/mol)	$\Delta E_{des}/100$ (kJ/mol)
H_2 dissociative adsorption	0.016	0.25[b]	0.42[b]
C_2H_2 adsorption	100.0	0.00[c]	1.21[c]
C_2H_4 adsorption	100.0	0.00[c]	0.63[c]

[a] Evaluated as the ratio between the number of molecules colliding, from the vapour phase, with the catalyst surface with energy in the range within the values of the activation energy of adsorption, ΔE_{ads}, and the activation energy of desorption, ΔE_{des}, and the total number of the colliding molecules. The energy possessed by the striking molecules is determined by randon number generator that works by referring to Maxwell energy distributions
[b] Evaluated by quantum mechanical calculations [19]
[c] Taken from Ref. [21]

Table 3. Activation energies to be employed for calculating the frequencies of occurrence, per second per site, of the steps involved in the title reaction

Process	$\Delta E/100$ (kJ/mol)
H diffusion	0.04[a]
C_2H_2 diffusion	0.24[b]
C_2H_3 diffusion	0.18[c]
C_2H_4 diffusion	0.13[b]
C_2H_5 diffusion	0.06[c]
C_2H_6 diffusion	0.00[b]
$C_2H_n(*)_2 + H(*) \rightarrow C_2H_{n+1}(*)_2 + *$	0.35[d]
$C_2H_{n+1}(*)_2 + H(*) \rightarrow C_2H_{n+2}(*)_2 + *$	0.49[d]
$C_2H_{n+1}(*)_2 + * \rightarrow C_2H_n(*)_2 + H(*)$	0.43[d]
H_2 desorption	0.42[a]
C_2H_2 desorption	1.21[e]
C_2H_4 desorption	0.63[e]
C_2H_6 desorption	0.00[e]

[a] Evaluated by quantum mechanical calculations [19]
[b] Estimated as 20% of the desorption activation energy [22]
[c] Activation energy of diffusion probabilities of C_2H_{m+1} is obtained by averaging the activation energies of diffusion of C_2H_m and C_2H_{m+2} ($m = 2, 4$)
[d] See Ref. [12] and text, $n = 2, 4$
[e] Taken from Ref. [21]

temperature were changed to reproduce the experimental conditions [7] to be simulated. In the simulations almost all the surface events were guided [24] by a preliminary diffusion event.

Fixed the reactant pressures and temperature, the event probabilities are automatically adjusted and used by the tdMC algorithm. In fact, probabilities are determined by the activation energy of the events; however, the ideal value of the activation energy of an event that was found, for example, by quantum mechanical calculations, could be modified by the surrounding surface species deposited around the sites on which the event is occurring [12]. These effects are automatically arranged by tdMC. The algorithm also displays and mimics the way in which the activation energies of the surface processes are influenced by the available surface energy (ASE) distributions that originate on the catalyst surface by the changes in the metallic properties [4, 12] of the catalyst crystallites.

Here, the concept of catalyst metal dispersion [4, 5], Dx, is used. Dx is the ratio between the number of the exposed atoms (surface atoms) of the catalyst particles and the number of all the atoms (surface and bulk atoms) constituting the same particles. Dx is inversely proportional to the average gyration radius [25] of the particles and so to the size of the same particles.

Since higher metal dispersion corresponds to higher metal exposure, it could seem that the catalyst activity should increase when increasing Dx; however, on increasing Dx the particle sizes decrease and reach values for which metal properties are lost and dramatic and not easily predictable changes [4, 5, 12] in the catalyst activity are observed. Finally, the formation of surface deposits could also have different effects with respect to the changes in the particle sizes.

3 Results and discussion

There is no uniformity of insight [1, 4, 5, 26] into the interpretation of the results concerning the influence of the metal dispersion of the catalyst crystallites on their catalytic activity and selectivity. The difficulties of explanation arise from the existence of many factors involved in the surface reactions. Some of these have been summarised in the previous section. In fact, the change in particle sizes of the supported metal crystallites modifies both the ratio of the different surface sites and the electronic properties of the particles [4]. The effects of these modifications are convoluted together and are also influenced by several effects. These are due to the metal particle shape reorganisation [27] and to the morphological and electronic changes occurring on the metal surface which originate from the interaction of the crystallites with the support and with the reagents [12]. Of course, by experimental approaches, it is not easy to evaluate the different contribution of the previously mentioned factors and thus to solve the apparent experimental inconsistencies of the dependence of catalyst selectivity and activity caused by the metal dispersion.

The simulative approaches allow one to separate the different microscopic contributions. In particular, it is possible to evaluate separately the effects of the surface deposits [7, 8, 28] and of the ASE distribution on the simulated reaction. Hence a deconvolution of the geometric influences, i.e. of the changes in the ratio of the different surface sites, from the electronic and decorative effects on the catalyst activity can be performed. Moreover, due to the stability of the catalysts [7, 29] employed in the mimicked experiments, the metal particle shape reorganisation can be excluded.

On a given face, it is possible to distinguish [4] surface **s**, edge **e** and corner **c** sites, whose relative amounts change with Dx (Scheme 1a). Edge and corner, shared between two and three surfaces, respectively, are border sites. We may assume [19] that the species occupying border sites can interact with the species coming from

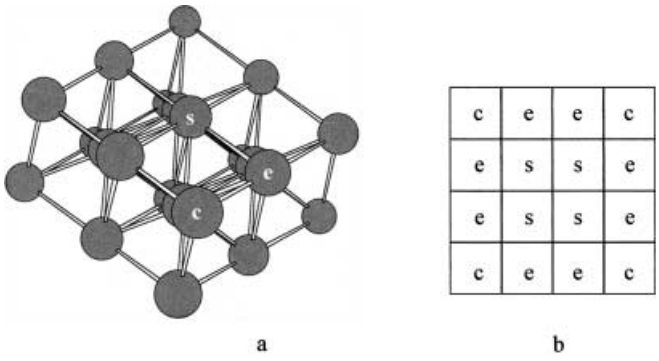

Scheme 1

just one of the neighbouring surfaces. In this case, it is possible to characterise the different class of sites as shown in Scheme 1b, where a model of a {100} metal face is represented.

Consequently, surface, edge and corner sites, if electronic and/or decorative effects are not present, differ only for the number of their neighbouring sites (in a {100} face, 4, 3 and 2, respectively), and so for their accessibility. In a boundary-conditioned square matrix, for instance, a {100} metal face (Scheme 2a), we may modify the accessibility to the sites by inserting gaps (g) into the surface (Scheme 2b). Gaps are not accessible to any species and like the empty sites are not sterically hindered.

This procedure allows us to introduce edge and corner equivalent sites. So, considering a surface matrix with an appropriate number of gaps, it is possible to mimic different values of Dx.

The molar ratios of the distinct surface sites have been calculated [4] for cubic–octahedral particles having different metal dispersion. The cubic–octahedral geometry is particularly suitable to model metal particles because, like the real metal crystallites, it displays just {100} and {111} faces. The values of the site molar ratios and the corresponding Dx calculated for cubic–octahedral particles and for a 100×100 surface matrix modified by random introductions of given percentages of surface gaps are shown in Table 4. Table 4 shows that it is possible to introduce on the surface matrix percentages of surface gaps able to reproduce site molar ratios typical of given metal dispersions: 10% of gaps on the surface correspond, for example, to the site molar ratios of crystallites with Dx = 0.31. Hence, for the surface matrix, it is possible to define a kind of Dx equivalent to be used for mimicking the effects of a metal dispersion on the catalyst activity and selectivity. The sum of the site molar ratios of the modified surface matrix is slightly lower than 1 for gap amounts larger than 5%. This depends on the presence of sites surrounded by four gaps which, given the very low number, have not been taken into consideration.

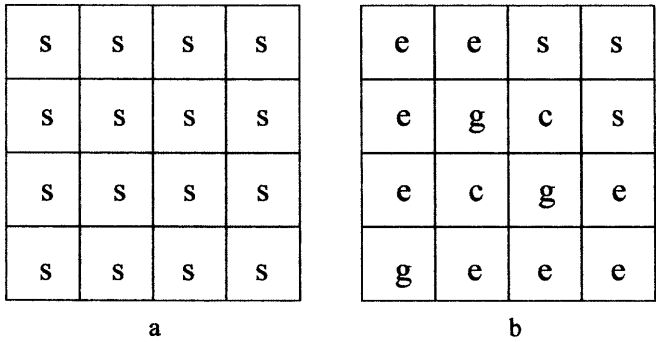

Scheme 2

The simulated reactions were performed experimentally [7] on a Pd/pumice catalyst employing front- and tail-end mixtures. The catalysts used were obtained by sintering, at different temperatures under hydrogen flow, a basis Yermakov [29] catalyst containing 0.05% of Pd. These Pd/pumice catalysts contain crystallites having spherical symmetry [29] and very likely cubic–octahedral shape. Due to the method of synthesis of the catalysts, their metal content was constant. Also the catalyst density, after sintering was constant, whereas Dx ranged between 0.05 and 0.65.

TOF values for the acetylene conversion [7], $TOF_{C_2H_4}$, at 298 K, for both front- and tail-end mix-

Table 4. Surface molar ratio ($\chi \mathbf{x}_G$) at different metal dispersion (Dx) of cubic–octahedral crystallites and equivalent surface molar ratio of a 100×100 surface matrix ($\chi \mathbf{y}_R$) for different gap percentages (% *gaps*) randomly introduced on a {100} surface. **x** is a generic site of the geometrically (G) regular crystallites. **y** is an equivalent generic site obtained by random (R) introductions of gaps on the equivalent surface matrix. Surface, edge and corner sites, are represented by s, e and c, respectively. Dx was determined by small-angle X-ray scattering [7]

Dx	χs_G	χe_G	χc_G	% gaps	χs_R	χe_R	χc_R
0.09	0.91	0.09	0.00	2.5	0.91	0.09	0.00
0.16	0.81	0.17	0.02	5.0	0.81	0.17	0.02
0.31	0.66	0.31	0.03	10.0	0.66	0.29	0.04
0.41	0.53	0.40	0.07	15.0	0.53	0.36	0.09
0.51	0.44	0.46	0.10	20.0	0.44	0.42	0.12
0.62	0.35	0.50	0.15	25.0	0.35	0.46	0.17

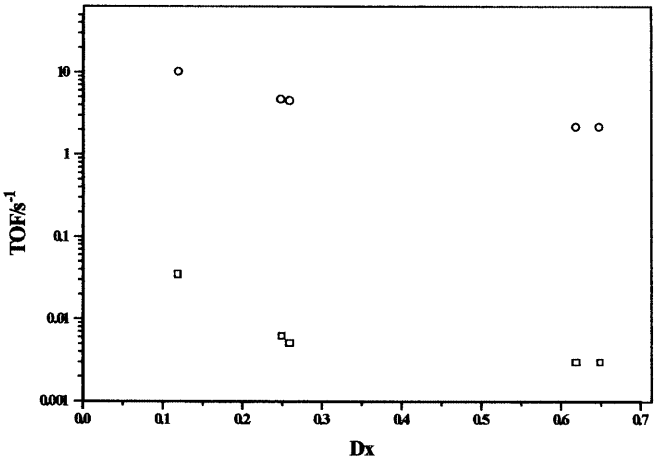

Fig. 1. Turnover frequency of acetylene conversion ($TOF_{C_2H_4}$) versus catalyst metal dispersion (Dx) hydrogenation of front-end (○) and tail-end (□) mixtures at atmospheric pressure on Pd/pumice catalysts having equal density and metal loading at 298 K

tures, are reported in Fig. 1. Although the shapes of the curves are similar, there is a difference of about 2 orders of magnitude between the $TOF_{C_2H_4}$ values obtained employing tail- and front-end mixtures on the same Pd/pumice catalysts.

S_E at a fixed temperature showed [7] a dependence on the amount of acetylene converted and on the characteristics of the mixtures. Conversely, S_E was not dependent [7] on the metal dispersion of the catalyst employed. The experimental activity and selectivity data were collected at a corresponding acetylene conversion lower than 20%. In this case the experimental S_E was invariably about 40%, independent of the feedstock mixture considered.

By employing the parameters of Tables 1–3, the catalytic activity mimicked by metal surfaces having similar molar ratios of the different surface sites but different numbers of catalytic sites was proportional to the number of the catalytic sites. This fact assures [12] that tdMC, for the differently modified surface matrix, always works in chemical regime [7, 30] conditions.

Experimental and simulated $TOF_{C_2H_4}$ versus Dx curves for front- and tail-end mixture hydrogenation, are shown in Figs. 2 and 3, respectively. The total pressure (1 atm) and temperature (298 K) in the experimental and the simulated hydrogenation were the same in the front- and tail-end systems. Also the activation energies of the steps used in the simulations of the two systems were the same.

Figures 2 and 3 show that tdMC reproduces properly the order of magnitude of $TOF_{C_2H_4}$ both in front- and in tail-end mixture hydrogenation. The values of S_E were roughly constant in the range of Dx considered for the two reaction systems; however, the simulated S_E values were rather different, in both front- and tail-end mixtures, from the experimental ones. Moreover, Figs. 2 and 3 show that the shapes of the curves obtained by experimental and simulated activity points are somewhat different. Furthermore, the same figures reveal that

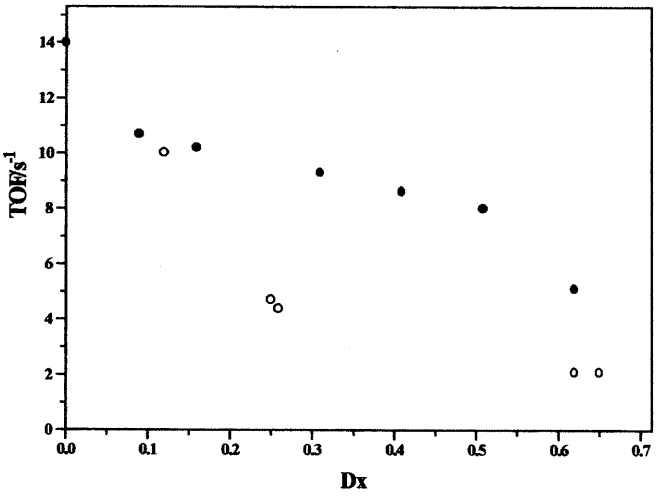

Fig. 2. Hydrogenation of a front-end mixture (hydrogen, acetylene and ethylene partial pressure, 0.637, 0.0050 and 0.358 atm respectively) on Pd/pumice catalysts at 298 K: $TOF_{C_2H_4}$ versus. Dx, experimental (○) and simulated (●) points

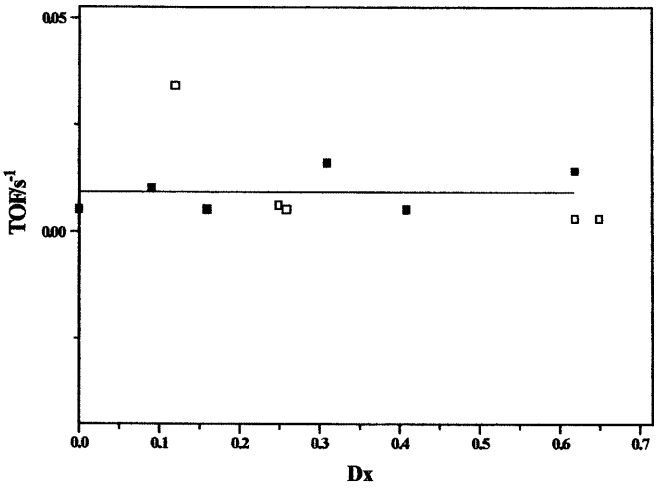

Fig. 3. Hydrogenation of a tail-end mixture (hydrogen, acetylene and ethylene partial pressure, 0.0056, 0.0029 and 0.9915 atm respectively) on Pd/pumice catalysts at 298 K: $TOF_{C_2H_4}$ versus Dx, experimental (□) and simulated (■) points. The *horizontal line* indicates the mean value of the simulated $TOF_{C_2H_4}$

simulated and experimental activity points do not show any simple correlation with the variation of the site molar ratios observed when changing Dx (Table 4).

These observations constitute a direct proof that, at least for the title reaction, just geometric considerations are not able to explain the connection between catalytic activity–selectivity patterns and catalyst particle sizes. It is our opinion that this conclusion could be broadly extended to all the surface reactions and that studies attempting correlation between activity and metal dispersion, based only on geometric considerations, must be considered very carefully.

It has been found that both ASE distribution [12] and decoration effects [7, 8, 12] due to surface species can dramatically modify the properties of a catalytic surface. Given the range of the metal dispersion of the Pd/pumice catalysts considered and the spherical shape of the metallic crystallites, the metal particle sizes should range between about 2 and about 8 nm, so these particles have typical [4] metallic properties. Therefore, for these catalysts we should not observe variations in the ASE distribution related to modifications of the metal properties [12] of the particles.

Conversely, it was found that in Pd/pumice catalysts, strong interactions of the crystallites with the support could induce changes in the electronic properties of the metallic particles [31]. Moreover, the growing of surface carbonaceous species [7–9, 12, 28, 32] could also modify the metal surface activity by their steric interaction [12, 32] with the surface species and by the transformations induced on the electronic band of the metal particles.

The data presented allow one to hypothesise [12] that the different surface sites have different ASE values. It is interesting to mention that different values of electronic charge were found on surface, edge and corner sites by ab initio quantum mechanical calculation [19]. The ASE distributions [12] and the steric hindrance energy due to surface species interactions are very likely to change with

the metal dispersion and could cause the observed differences between experimental and simulated results. To test this hypothesis, we performed fitting procedures by tdMC simulations [12] on front- and tail-end mixtures at the pressure and temperature of the simulated experimental data [7] (for details see also captions of Figs. 2, 3). In the simulations, surface, edge and corner sites could be covered by a variable percentage of carbonaceous deposits and could have a nonuniform ASE.

To obtain fit parameters the following function was minimised by using the simplex AMOEBA from Ref. [16]:

$$F = \frac{1}{n}\sum_{i=1}^{n}\left|\frac{\delta_{p_i}}{\varepsilon_{p_i}}\right| , \quad (4)$$

where n is the number of experimental points of $TOF_{C_2H_4}$ reproduced by tdMC, whereas δ_{p_i} and ε_{p_i} are the differences found between simulated and experimental results and the averaged experimental error of the ith point, respectively. Values of F close to or smaller than 1 should constitute a validation of the fitting model.

In the fitting procedure we imposed the value of the steric hindrance parameter of the carbonaceous deposits. Assuming that the carbonaceous deposits were freshly formed, hence not dehydrogenated, their steric hindrance parameter was fixed between those of acetylene and ethylene (0.15). Then, the parameters introduced in the fitting procedure were the activation energy values of the three kinds of sites and the percentage of the surface sites covered by the carbonaceous deposits. These parameters were considered as variable and nonvariable with the two different reaction mixtures, respectively.

The percentages of the surface carbonaceous deposits at different Dx were introduced before starting the simulations. The correctness of this procedure is supported by the experimental findings that the activity–selectivity patterns of these catalytic systems do not change even if the reaction is stopped and then restarted after a light cleaning of the surface [7], which is not able to change the surface deposit population.

In the fit, to simplify the interpretation of the results, the activation energy parameters of the events were represented as the sum of two terms. The first of these, for a given event, is an activation energy value involved in the same event and is reported in Tables 2 and 3, whereas the second is a variable energetic term. The latter, reported in Table 5 as ΔE (energetic fit parameters), is fixed for a given kind of surface site, irrespective of the metal dispersion, but it is different for different surface sites. These energetic terms are related to the ASE of the different sites. The difference between the refined and the original (reported in Tables 2, 3) activation energy parameters gives ΔE values.

Considering in Eq. 4, ε_{p_i} at the different experimental Dx to be invariably equal to 7.5%, resulted in F values of 0.65 and 0.90 for tail- and front-end mixtures respectively. This result shows that on average the difference between simulated and experimental results is smaller than the error in the same experimental results.

For a given reaction mixture the percentage of the surface sites covered by carbonaceous deposits was almost constant with respect of the metal dispersion; however, its value was quite different for the two reaction mixtures, about 25–30% and 10–15% for the front- and tail-end mixtures, respectively. Significantly, simulated S_E in the range of Dx considered, in accordance with the experimental findings, showed values between 35 and 50% both in front- and in tail-end mixtures.

The energetic fit parameters, ΔE_F and ΔE_T, of the different kinds of sites are reported in Table 5. The values of ΔE_F and ΔE_T must be considered as average values of the various reaction events. Speculation on the origin of ΔE leads us to hypothesise that a mechanism of accumulation–release of energy is present on every surface site. A heuristic microscopic explanation of these accumulation–release phenomena is actually performed by the "sandpile model" [33] of Bak. The energy involved could be due to the reaction environment [12], whereas the energy relaxation time could be due to the electronic characteristic of the surface sites.

The difference between ΔE found for the same kind of sites for the two reaction mixtures would suggest that, besides the metallic characteristics, the electronic properties of the surface sites could also be influenced by the interaction between the metal surface and absorbed species.

As shown in Table 6, the simulated catalytic activity to acetylene hydrogenation due to the fit adjustments both in tail- and in front-end mixtures was modulated by the change in the hydrogen surface molar ratio. However, hydrogen is also needed to obtain, from acetylene–ethylene mixtures, polymer species among the products and on the catalyst surface, i.e. formation of surface

Table 5. Energy fit parameters on the different surface sites. ΔE_F and ΔE_T are the difference, considering front- and tail-end mixtures, respectively, between the values of the activation energies used in the best-fit simulations and those of Tables 2 and 3

Site	ΔE_T/ (kJ/mol)	ΔE_F/ (kJ/mol)
s	−0.05	−0.03
e	0.16	0.71
c	−0.35	−1.89

Table 6. Ratio of the values determined before and after the fit refinements of the activity, expressed as the turnover frequency of acetylene conversion ($TOF_{C_2H_4}$), and of the corresponding hydrogen surface population at different metal dispersions. $\rho TOF_{C_2H_4}$ is the ratio between the $TOF_{C_2H_4}$ values obtained by simulations performed with the parameters of Tables 2 and 3 modified by the fitting procedure and those achieved by simulations which employed the unrefined parameters of the same tables. $\rho\theta_x$ is the ratio between the X species surface populations, generated by simulations taking and not taking into account the fit refinements

Dx	Front-end mixture			Tail-end mixture		
	$\rho TOF_{C_2H_4}$	$\rho\theta_H$	$\rho\theta_{C_2H_4}$	$\rho TOF_{C_2H_4}$	$\rho\theta_H$	$\rho\theta_{C_2H_4}$
0.09	1.0	1.0	1.1	4.4	1.8	3.5
0.31	0.4	0.5	1.2	0.4	0.5	1.4
0.62	0.4	0.4	1.2	0.3	0.3	1.2

carbonaceous deposits. Accumulation of polymers occurs in parallel with hydrogenation. Since the experimental data were collected in about the same reaction time [7], opposite to what has already been observed [34], the results of the simulations show that the parallel reactions are more competitive with the hydrogenation for a higher hydrogen amount present among the reagents. This apparent inconsistency can be exploited considering that all the reagent ratios change in the two feedstock mixtures considered when changing the hydrogen amount.

However, the rate of the parallel surface polymerisation is much lower than that of hydrogenation, (see before, stop and restart experiment). For this reason the title reaction can be studied in the pseudo-steady state also if it occurs in transient surface conditions. The surface molar ratios determined by simulated reaction of front- and tail-end mixtures on ideally zero dispersed Pd catalyst are reported in Table 7. The partial pressure of the reagents and temperature are the same as previously employed. The molar ratios are obtained with or without consideration of the refinements due to the fitting procedures. They clearly illustrate that due to the formation of surface polymers, a decrease in the amount of ethylene and an increase in the amount of acetylene occur on the surface.

We think that polymers on the surface are produced from acetylene and ethylene, their steric hindrance and that of the formed surface polymers driving the adsorption of further hydrocarbons, giving rise to the surface population described in Table 7.

Interestingly, the ethylene surface molar ratio is the largest one. Although this occurred, S_E was always close to 40%. This fact indicates that acetylene is in some way more reactive than ethylene.

In fact, the carbonaceous deposits increase [12] the surface amount of acetylene and, hence, the activity of the catalyst to the acetylene hydrogenation; however, since the ethylene–acetylene surface ratios are larger than 1, the previously mentioned condition is not able to justify the experimental S_E. Moreover, due to the activation energies involved in the hydrogenation–dehydrogenation processes (in the previous section assumed to be similar for ethylene and acetylene), S_E cannot depend on those energetic factors.

It is very likely that S_E is driven by surface decoration phenomena. In fact, on analysing the surface matrix at the steady state it is observed that acetylene species and polymeric deposits wrap up ethylene and eventually ethyl. For this reason, ethylene and ethyl appear to be isolated on the catalyst surface and are very likely to have less probability than the other hydrocarbons resident on the catalyst surface of getting in contact with surface hydrogen. The reality of this picture cannot be definitely established by tdMC; however, the correct order of magnitude of S_E which is always found seems to suggest its correctness. If our interpretation were sound, the superiority of the Langmuir–Hinshelwood model with respect to the Eley–Rideal model for the title reaction would be established.

Fit-refined surface hydrocarbon ratios very similar to those of Table 7 were found in simulations of catalytic systems, either front- or tail-end mixtures, reacting on Pd catalysts having different Dx. We believe that this occurrence gives the invariability of S_E with respect of Dx and it is mainly due to the constant amount of carbonaceous deposits characterising, irrespective of the metal crystallite sizes, the catalyst surface.

However, it is found experimentally that for acetylene conversion exceeding 50% of the starting amount, S_E is always larger for the front-end than for the tail-end mixture [7]; therefore S_E, besides the surface carbonaceous deposits, must be correlated to the progress of the reaction because, with the acetylene conversion, the relative probability of hydrocarbon surface interaction varies together with the ratio of acetylene–ethylene in the vapour phase.

To summarise, by means of the electronic and steric effects occurring on the different surface sites of the metal crystallites, the growth of polymer deposits could control the hydrocarbon surface population (acetylene, ethylene, ethyl and vinyl species). In this way, although the amount of hydrogen in the vapour phase, and so on the surface catalyst, influences the speed of the hydrogenation processes, polymer deposits on the surface mainly govern the selectivity of the catalyst.

Finally, it is interesting to underline some aspects related to the connection between experimental and simulated points. The main discriminating criteria employed to collect the experimental TOF and S_E points [7], simulated in this work, were to be obtained in chemical regime conditions, conversion data in combination with a comparable amount of hydrogenated acetylene, following a constant preconditioning [7] and accumulating time. These facts and the results of the present work suggest that the kinetics of surface deposit growth is insensitive to Dx and more interestingly, that if we had modified the collecting criteria we would have certainly discussed different activity and selectivity curves.

Therefore, without considering the elementary details discussed here, and which are still certainly involved to various degrees in all the surface processes, we could get at least a misleading conclusion depending on the ex-

Table 7. Typical surface populations found on the metal surface when front- and tail-end mixtures react in the presence of Pd at atmospheric pressure and 298 K

Surface species	Front-end mixture		Tail-end mixture	
	θ° [a]	θ^{*} [b]	θ°	θ^{*}
Nothing[c]	0.0853	0.1064	0.3232	0.2780
H	0.3336	0.3304	0.0152	0.0281
$C_2H_2 + C_2H_3$[d]	0.0509	0.0560	0.0176	0.0656
$C_2H_4 + C_2H_5$[d]	0.5288	0.2320	0.6440	0.4783
C_xH_y[e]	0.0000	0.2750	0.0000	0.1500

[a] Surface molar ratios on ideally zero dispersed metal, simulated without considering the parameters refined by fitting procedures
[b] Surface molar ratios on ideally zero dispersed metal, simulated considering the parameters achieved by fitting procedures
[c] i.e. empty sites
[d] C_2H_3 and C_2H_5 surface molar ratios had almost no effect on the total amount
[e] Carbonaceous deposits

perimental procedures adopted. While this subject, we ought to mention that either higher or lower catalytic activities and activity–selectivity patterns of the title reaction can be easily and completely framed in the surface reactivity model presented just by changing the numerical values of the simulating parameters and, hence, the experimental environments mimicked. In this way, we should also be able to justify the fragmentary [5–10] behaviour shown in analogous reaction contexts.

4 Conclusion

This study shows that the elementary physical phenomena convoluted in the activity–selectivity patterns of a catalytic system are many and complex. In particular, it is pointed out that the activity and selectivity of Pd catalysts having different metal dispersions employed to transform acetylene–ethylene front- and tail-end mixtures are strongly influenced by

- The geometrical characteristics of the surface sites.
- The electronic properties of the surface sites.
- The surface population.
- The formation of surface carbonaceous deposits usually not considered as part of the catalytic process.
- The geometrical characteristics of the agglomerate designed on the catalyst surface by the different species involved.
- The electronic properties of the surface species.
- The mutual complex interaction, changing with the reaction progress time, of each of the above points with all the others.

Computing and simulation approaches seem to have a sound chance of success in the analysis of these complicated systems. In detail, tdMC supported by quantum mechanical calculations, employing a unique model irrespective of the reaction mixtures driven by simple elementary events and by the concepts of the steric hindrance parameter and the ASE already introduced was able to account for the microscopic speculation and the macroscopic evidence concerned with the title reaction.

However, tdMC must be considered just as a convolution system, which is able to mix the elementary properties we are taking inside. In performing this, from local information, such as the activation energy involved in the ethylene hydrogenation on a surface site ensemble, we get mass information, i.e. the convolution of much local information, and incidentally other local information otherwise not attainable, such as the ASE value on a given site.

Ultimately, different experimental procedures could dramatically modify the activity–selectivity patterns of a catalytic system. Microscopic computing approaches, such as tdMC, can interpret the changes occurring by modifications of the experiment and can get more information on them. In contrast, other more classic interpretative macroscopic models, not taking into consideration microscopic details, could be seriously challenged by the same modifications of the experiment.

References

1. (a) Gigola CE, Aduriz HR, Bodnariuk P (1986) Appl Catal 27: 133; (b) Aduriz HR, Bodnariuk P, Dennehy M, Gigola CE (1990) Appl Catal 58: 227
2. Weiss AH, Gambhir BS, La Pierre RB, Bell WK (1977) Ind Eng Chem Proc Res Dev 16: 352
3. Boitiaux JP, Cosins J, Derrien M, Léger G (1985) Hydrocarbon Process 3: 51
4. Bond GC (1991) Chem Soc Rev 20: 441
5. (a) Che M, Bennet CO (1989) Adv Catal 36: 55; (b) Sàrkàny A, Weiss AH, Guczi L (1986) J Catal 98: 550; (c) Duca D, Liotta LF, Deganello G (1995) J Catal 54: 69; (d) Duca D, Liotta LF, Deganello G (1995) Catal Today 24: 15
6. (a) Gutman H, Lindlar H (1969) In: Viehe HG (ed) Chemistry of acetylene. Dekker, New York, p 355; (b) Aduriz HR, Bodnariuk P, Coq B, Figueras F (1991) J Catal 129: 47; (c) Nørskov JK (1993) In: King DA, Woodruff DP (eds) The chemical physics of solid surfaces, vol 6. Elsevier, Amsterdam, p 22
7. (a) Duca D, Frusteri F, Parmaliana A, Deganello G (1996) Appl Catal A 46: 269; (b) Duca D, Arena F, Parmaliana A, Deganello G (1998) Appl Catal A 172-II: 207
8. Borodzinski A, Golebiowski A (1997) Langmuir 13: 887
9. (a) Thomson SJ, Webb G (1976) J Chem Soc Chem Commun 1976: 526; (b) Mc Gown WT, Kemball C, Whan DA, Scurrell MS (1977) J Chem Soc Faraday Trans 73: 632; (c) Al-Ammar AS, Webb G (1978) J Chem Soc Faraday Trans 74: 195; (d) Al-Ammar AS, Webb G (1978) J Chem Soc Faraday Trans 74: 657; (e) Al-Ammar AS, Webb G (1979) J Chem Soc Faraday Trans 75: 1990; (f) Margitfalvi J, Guczi L, Weiss AH (1981) J Catal 72: 185; (g) Berndt GF, Thomson SJ, Webb G (1983) J Chem Soc Faraday Trans 79: 195; (h) Moses JH, Weiss AH, Matusek K, Guczi L (1984) J Catal 86: 88; (i) Pestman R, den Hartog AJ, Ponec V (1990) Catal Lett 4: 287; (j) Houzvicka J, Pestman R, Ponec V (1984) Catal Lett 30: 289; (k) Asplund S, Fornell C, Holmgren A, Irandoust S (1995) Catal Today 24: 181; (l) Asplund S (1996) J Catal 158: 267
10. (a) Duca D, Botár L, Vidóczy T (1996) J Catal 162: 260; (b) Duca D, Baranyai P, Vidóczy T (1998) J Comput Chem 19: 396
11. Garrison BJ, Kodali PBS, Srivastava D (1996) Chem Rev 96: 1327
12. Duca D, La Manna G, Russo MR (1999) Phys Chem Chem Phys 1: 1375
13. Ziff RM, Gulari E, Barshad Y (1987) Phys Rev Lett 56: 2553
14. Dong W, Kresse G, Hafner J (1997) J Mol Catal 69: 119
15. (a) Ehsasi M, Matloch M, Frank O, Block JH, Christmann K, Rys FS, Hirshwald W (1989) J Chem Phys 91: 4949; (b) Boudart M, Djéga-Mariadassou G (1984) Kinetics of heterogeneous catalytic reactions. Princeton University Press, Princeton, p 155
16. Press WH, Teukolsky SA, Vetterling WT, Flammery BP (1992) Numerical recipes. Cambridge University Press, Cambridge
17. Battiston GC, Dalloro L, Tauszik GR (1982) Appl Catal 2: 1
18. Dumesic JA, Rudd DF, Aparicio LM, Rekoske JE, Treviño AA (1993) The microkinetics of heterogeneous catalysis. ACS Professional Reference Book. American Chemical Society, Washington, DC
19. La Manna G, Barone G, Varga Zs, Duca D (1999) J Mol Catal (submitted)
20. Yasumori I, Shinohara H, Inoue Y (1973) In: Proc V Int Congr Catal – Palm Beach 1972. North-Holland, Amsterdam, p 53/1
21. Bertolini JC, Massadier J (1984) In: King DA, Woodruff DP (eds) The chemical physics of solid surfaces, vol 3B. Elsevier, Amsterdam, p 133
22. Atkins PW (1994) Physical chemistry, 5th edn. Oxford University Press, Oxford, p 996
23. Hlavathy Z, Tétényi P, Paál Z (1992) J Chem Soc Faraday Trans 88: 2059
24. (a) Kaya H, Erzan A, Kadirgan F (1993) J Chem Phys 98: 9030; (b) Bowker M, Leibsle F (1996) Catal Lett 38: 123; (c) Allen CE, Seebauer G (1996) J Chem Phys 104: 2557

25. Guinier A, Fournet G (1959) Small-angle scattering of X-rays. Chapman & Hall, London
26. Hub S, Hilaire L,Toroude R (198) Appl Catal 27: 307
27. Resuyanskii ED, Myshlyavtsev AV, Elokhin VI, Balzhinimaev BS (1997) Chem Phys Letters 264: 174
28. (a) Rajaram J, Narula APS, Chawla HPS, Dev S (1983) Tetrahedron 13: 2315; (b) Aramendia MA, Boran V, Imenez C, Marinas JN, Sempere ME, Urbano FJ (1990) Appl Catal 63: 375
29. Fagherazzi G, Benedetti A, Deganello G, Duca D, Martorana A, Spoto G (1994) J Catal 150: 117
30. Madon JR, Boudart M (1982) Ind Eng Chem Fundam 21: 438
31. Venezia AM, Rossi A, Duca D, Martorana A, Deganello G (1995) Appl Cat A 125: 113
32. Bond GC (1997) Appl Catal A 149: 3
33. Bak P (1997) How nature works. Oxford University Press, Oxford
34. Duca D, La Manna G, Deganello G (1998) Catal Lett 52: 73